

3D Face Recognition with Sparse Spherical Representations[☆]

R. Sala Llonch^a, E. Kokiopoulou^b, I. Tasic^b, P. Frossard^b

^a*Hospital Clinic - Universitat de Barcelona, 08028 Barcelona, Spain.*

^b*Signal Processing Laboratory (LTS4), Ecole Polytechnique Fédérale de Lausanne (EPFL), Lausanne 1015, Switzerland.*

Abstract

This paper addresses the problem of 3D face recognition using simultaneous sparse approximations on the sphere. The 3D face point clouds are first aligned with a novel and fully automated registration process. They are then represented as signals on the 2D sphere in order to preserve depth and geometry information. Next, we implement a dimensionality reduction process with simultaneous sparse approximations and subspace projection. It permits to represent each 3D face by only a few spherical functions that are able to capture the salient facial characteristics, and hence to preserve the discriminant facial information. We eventually perform recognition by effective matching in the reduced space, where Linear Discriminant Analysis can be further activated for improved recognition performance. The 3D face recognition algorithm is evaluated on the FRGC v.1.0 data set, where it is shown to outperform classical state-of-the-art solutions that work with depth images.

Key words: Sparse representations, dimensionality reduction, spherical representations, 3D face recognition.

1. Introduction

Automatic recognition of human faces is an actively researched area, which finds numerous applications such as surveillance, automated screening, authen-

[☆]This work has been partly supported by the Swiss National Science Foundation, under grants NCCR IM2 and 200020-120063.

the sphere.

The spherical face signals then undergo a dimensionality reduction step that represents each face with a reduced set of discriminant features. We build a dictionary of functions on the sphere and we select the discriminant basis functions by simultaneous sparse approximations. The face signals are finally projected onto the resulting reduced subspace, in order to generate feature vectors. We finally implement a recognition step where Linear Discriminant Analysis (LDA) is performed on the subspace representation of the faces. The recognition system is illustrated on Fig. 1, where $s_i(\theta, \phi)$ denotes the spherical signal s_i as a function of position (θ, ϕ) on the 2D sphere, and c_i is a feature vector.

The performance of the 3D face recognition system is evaluated on the FRGC v.1.1.0 data set. The proposed algorithm outperforms state-of-the-art solutions based on Principal Component Analysis (PCA, [5]) or Linear Discriminant Analysis (LDA) on depth images. Our fully automatic system provides effective classification performance that shows that 3D face recognition with spherical representations certainly represents a promising solution for person identification.

The paper is organized as follows. We provide an overview of the related work in 3D face recognition in Section II. Section III describes the automatic face registration process that permits to align the 3D points clouds before analysis. The dimensionality reduction step with simultaneous sparse approximations on the sphere is presented in Section IV and experimental results are finally provided in Section V.

2. Related work

3D face recognition has attracted a lot of research efforts in the past few decades due to the advent of new sensing technologies and the high potential of 3D methods for building robust systems with invariance to head pose and illumination variations. We review in this section the most relevant work in 3D face recognition, which can be categorized in methods using point cloud rep-

representations, depth images, facial surface features or spherical representations respectively. Surveys of the state-of-the-art in 3D face recognition are further provided in [2, 3].

The recognition methods that work directly on 3D point clouds consider the data in their original representation based on spatial and depth information. A priori registration of the point clouds is commonly performed by ICP algorithms [4, 6]. The classification is generally based on the Hausdorff distance that permits to measure the similarity between different point clouds [7]. Alternatively, recognition could be performed with “3D eigenfaces” that are constructed directly from the 3D point clouds [8]. The main drawback of the recognition methods based on 3D point clouds however resides in their high computational complexity that is driven by the large size of the data.

Many recognition systems use depth or range images that permit to formulate the 3D face recognition as a problem of dimensionality reduction for planar images, where each pixel value represents the distance from the sensor to the facial surface. Principal Component Analysis (PCA) and “Eigenfaces” can be used for dimensionality reduction [9], where the basis vectors are however typically holistic and of global support. PCA can be combined with Linear Discriminant Analysis (LDA) to form “Fisherfaces” with enhanced class separability properties [10]. Alternatively, dimensionality reduction can be performed via variants of non-negative matrix factorization (NMF) algorithms [11, 12, 13] that produce part-based decompositions of the depth images. Part-based decompositions based on non-negative sparse coding [14] have recently been shown to provide improved recognition performance than NMF methods in face recognition [15]. Recent methods have proposed to concentrate dimensionality reduction around facial landmarks like the nose tip [16] or in multiple carefully chosen regions [17] or to compute geodesic distances among the selected fiducial points [18]. They however require a selection of the fiducial points or areas of interest that is often performed manually and prevents the implementation of fully automatic systems.

Facial surface features have also been proposed for 3D face recognition. The

idea of recognizing 3D faces using curvature descriptors has been originally introduced in [19], where features are chosen to represent both curvature and metric size properties of faces. More recently, level sets of the depth function on range image have been used to define sets of facial curves [20]. They are further embedded in an appropriately defined shape manifold and compared based on geodesic distances. Facial curve representations provide global information about the whole facial surface, which unfortunately does not permit to take advantage of discriminative local features.

Finally, spherical representations have been used recently for modelling illumination variations [21, 22] or both illumination and pose variations in face images [23]. Spherical representations permit to efficiently represent facial surfaces and overcome the limitations of other methods towards occlusions and partial views [24]. To the best of our knowledge, the representation of 3D face point clouds as spherical signals for face recognition has however not been investigated yet. We therefore propose to take benefit of the robustness of spherical representations and of spherical signal processing tools to build an effective and automatic 3D face recognition system. We perform dimensionality reduction directly on the sphere, so that the geometry of 3D faces is preserved. The reduced feature space is extracted by sparse approximations with a dictionary of localized geometric features on the sphere that effectively capture spatially localized and salient 3D face features that are advantageous in the recognition process.

3. Automatic preprocessing of 3D face data

3.1. Automatic face extraction

We propose in this section a fully automatic preprocessing method for preparing and aligning 3D face point clouds before feature extraction and recognition. Unlike most of the algorithms in the literature, the preprocessing step does not require any manual intervention, which is an enormous advantage for the design of fully automated face recognition systems. The preprocessing scheme is

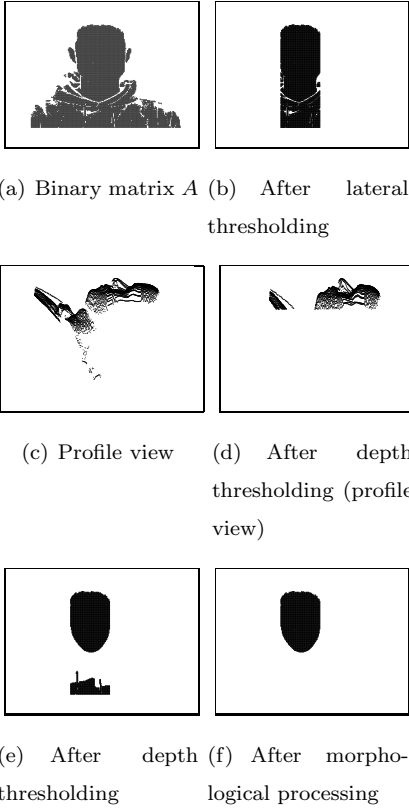


Figure 2: Main steps in facial region extraction

based on two main tasks, respectively the extraction of the facial region, and the registration of the 3D face. We present these tasks in more details in the rest of the section.

The main purpose of the face extraction step is to remove irrelevant information from the 3D point clouds, such as data that correspond to shoulder, or hair for example. The output of a facial scan typically forms a 3D point cloud $\{X, Y, Z\}$, where X and Y form a uniform Euclidean grid and Z provides the corresponding depth values. The point cloud is also accompanied by a binary matrix A of valid points, which has the same resolution as the grid implied by $X \times Y$. The nonzero pattern of such a sample binary matrix is shown in Fig. 2(a). There is however no guarantee that the points exclusively correspond to

face depth information, and face extraction is therefore necessary to ensure that the feature extraction concentrates on capturing discriminative facial information.

The first step in face extraction consists in removing data points on the subject’s shoulders. We estimate a vertical projection curve from the point cloud by computing the column sum of the matrix A . Then, we define two lateral thresholds on the left and right inflexion points of the projection curve, and we remove all data points beyond these thresholds, as illustrated in Fig. 2(b). We further remove the data points corresponding to the subject’s chest by thresholding of the histogram of depth values. It removes the data points with large depth values that are typically situated behind the data corresponding to frontal face information, as shown in Figs 2(c) and 2(d). We finally have to remove outlier points that remain in regions disconnected from the main facial area, as shown in Fig. 2(e). We therefore perform morphological image processing on the corresponding binary matrix A , where we keep only the largest region that typically correspond to the facial region, as presented in 2(f).

3.2. Automatic face registration

After extracting the main facial region from the 3D scans, the face signals have to be registered in order to ensure that all have the same pose before the recognition step. The registration typically applies rigid transformations on the 3D faces in order to align them. We propose a two-step approach for automatic registration, where an Average Face Model (AFM) is computed and then used for accurate registration.

First, we randomly pick a training face, and we align all the faces approximately to the sample face using the Iterative Closest Point (ICP) algorithm [4]. Given a model and a query point cloud, ICP computes a rigid transformation, consisting of rotations and translations, by minimizing the sum of square errors between the closest model points and query points. After coarse registration with ICP, the face signals are re-sampled on a uniform 2D grid using nearest neighbor interpolation. It permits to construct an AFM, by computing at each

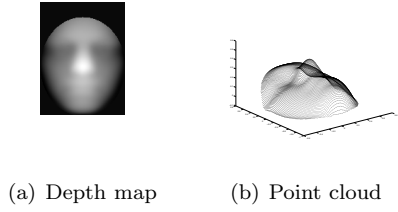


Figure 3: Average Face Model given as a depth map or a 3D point cloud.

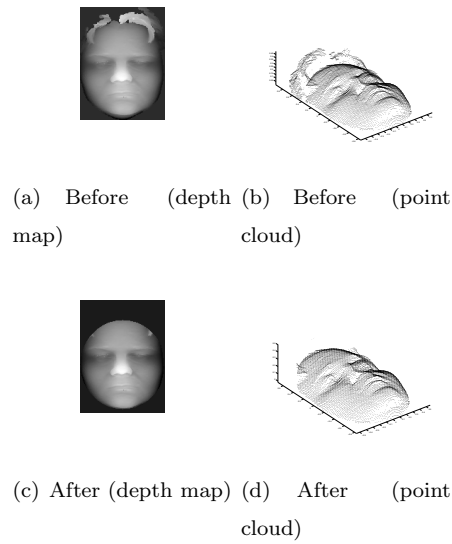


Figure 4: Illustration of ellipse cropping on depth maps and equivalent 3D point clouds.

grid point the average depth value among all training faces (see Figure 3) . The AFM is subsequently used as reference in order to define an ellipse that contains the main facial region. Since, the faces are already registered, this ellipse can be used to crop closely all faces in the training set. The ellipse cropping step removes all the irrelevant information that may be left over from the previous preprocessing steps, as shown in Figure 4.

A fine alignment of the faces can now be performed on the signals that have been cleaned from outliers. The accurate alignment is finally obtained by running ICP one more time. The AFM is now used as a reference face model, and all faces signals are registered with respect to the AFM.

4. Recognition with sparse spherical representations

4.1. Simultaneous sparse approximations

Efficient face recognition algorithms usually include a dimensionality reduction step, where high dimensional data are represented in a reduced subspace. We propose to use sparse signal representation methods for dimensionality reduction. Such methods have demonstrated good performance in 2D face recognition [25]. They present the advantage of capturing the main signal characteristics in a very small set of meaningful features, which are moreover defined a priori in a dictionary of functions. This presents an interesting advantage compared to classical methods such as PCA, whose feature vectors are data-dependent. In addition, a proper choice of the dictionary permits to build features that capture the geometrical information in the face signal. We give below a brief overview of sparse approximations, and we show later how we use them for dimensionality reduction on the sphere.

Let denote by $s_i, i = 1, \dots, N$, a set of functions in the Hilbert space \mathcal{H} . Let further denote by $\mathcal{D} = \{g_\gamma, \gamma \in \Gamma\}$ an overcomplete dictionary of unit L_2 norm functions indexed by γ , which spans the space \mathcal{H} . A function s_i has a sparse representation in \mathcal{D} if it can be represented in terms of a linear superposition of small set of basis functions $\{g_\gamma\} \in \mathcal{D}$. In other words, it can be expressed as $s_i = \Phi_{I_i} c_i$, where Φ_{I_i} denotes a matrix whose columns are atoms in $\mathcal{D}_{I_i} \subset \mathcal{D}$ that forms the sparse support of the signal s_i . The vector c_i represents the coefficients of the linear approximation of s_i with atoms in \mathcal{D}_{I_i} .

Finding the sparsest representation of a signal in a redundant dictionary \mathcal{D} is in general an NP-hard problem. Greedy algorithms like Matching Pursuit [26] have however shown to provide suboptimal yet efficient solutions with a limited computational complexity. It selects iteratively the functions from the dictionary that best matches the signals s_i . We have however to ensure that the atoms that form the support of the different signals s_i 's are identical, in order to permit to classify them in the feature space. Dimensionality reduction can thus be performed by simultaneous decomposition of all the signals $s_i, i = 1, \dots, N$.

Finding the sparse support \mathcal{D}_I that is common to all the signals $\{s_i\}$ can be achieved by the Simultaneous MP (SMP) [27] algorithm, which only induces a small increase of complexity compared to MP on a single signal [25]. In short, SMP greedily selects \mathcal{D}_I such that all the N functions s_i are simultaneously approximated in the same basis. It results in the extraction of K atoms such that all signals are simultaneously represented by linear combinations of them. Each signal can be re-written as $s_i = \Phi_I c_i$, where Φ_I denotes the matrix whose columns are the atoms in the common sparse support $\mathcal{D}_I \subset \mathcal{D}$. Finally, a few iterations are typically sufficient to capture most of the energy of the face signals to be approximated. It has been shown that residual error of the SMP approximation decays exponentially for correlated signals with the same support and additive white noise [27].

4.2. Spherical subspace selection with SMP

We propose to perform the classification of 3D face by dimensionality reduction on the sphere. We therefore project the 3D point cloud onto the unit sphere S^2 , and then we select a subspace that spans functions on S^2 . Since faces are typically star-shaped objects, spherical projection preserves the face geometry information, while reducing the classification complexity by mapping a 3D signal to a 2D spherical signal. Each face, given by a 3D point-cloud $\{p_n\} = \{(x_n, y_n, z_n)\}$ is, therefore, represented as a spherical function $r = s(\theta, \varphi)$ sampled at points $\{(r_n, \theta_n, \varphi_n)\}$, which are obtained by transforming Euclidean coordinates from the point cloud to spherical coordinates given by (θ, φ) that represent the elevation and azimuth angles.

Since we represent 3D faces as square-integrable functions on S^2 , denoted as $L^2(S^2)$, we can use the SMP to select a subspace of spherical basis functions as a dimensionality reduction step. We use a spherical dictionary proposed in [28], where the atoms are created by applying local geometric transforms to a generation function $g(\theta, \varphi)$ defined on the sphere. Local transforms include atom motion (τ, ν) (position on the sphere with respect to (θ, φ) , respectively), rotation ψ , and anisotropic scaling by two scales (α, β) in orthogonal directions. Motion



Figure 5: Gaussian atoms.

and rotation are realized using a rotation in $SO(3)$, which is the rotation group in \mathbb{R}^3 . Five transform parameters form the atom index $\gamma = (\tau, \nu, \psi, \alpha, \beta) \in \Gamma$, and the redundant dictionary is finally constructed by applying a large set of different γ 's to g . A detailed explanation of the dictionary construction is given in [28]. An example of the generating function is a 2-D Gaussian function in $L^2(S^2)$, given by:

$$g(\theta, \varphi) = \exp\left(-\tan^2 \frac{\theta}{2}\right). \quad (1)$$

Function in Eq.(1) represents an isotropic gaussian function, centered at the North Pole. In Figure 5 we show a few sample Gaussian atoms that are obtained by applying different local transforms to the generating function in Eq.(1).

Equipped with the spherical dictionary, we can directly apply SMP to find the common support of the spherical faces, where the inner product between two spherical functions $f = f(\theta, \varphi)$ and $g = g(\theta, \varphi)$ is however given by:

$$\langle f, g \rangle = \int_{\theta} \int_{\varphi} f(\theta, \varphi)g(\theta, \varphi) \sin \theta d\theta d\varphi. \quad (2)$$

In the following, we refer to this special case of SMP for spherical signals using the dictionary defined on the sphere, as *simultaneous spherical matching pursuit* (SSMP).

4.3. Recognition on the sphere

The algorithm for recognition of 3D faces on the sphere is finally illustrated in Figure 6. The first step performs dimensionality reduction, by projecting the spherical signals on the subspace spanned by the selected atoms i.e., $\text{span}\{\mathcal{D}_I\}$, as described above. If we denote the set of face signals by $S = [s_1, \dots, s_n]$, the SSMP performs the dimensionality reduction step by greedily selecting a

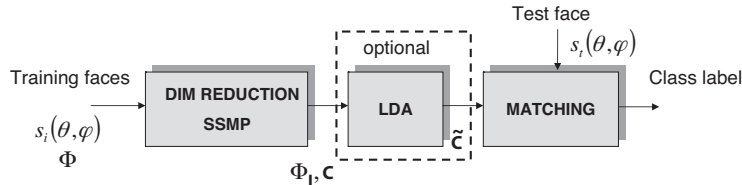


Figure 6: Block diagram of the recognition process.

set of K basis vectors $\mathcal{D}_I = \{g_{\gamma_1}, \dots, g_{\gamma_K}\}$ from the dictionary \mathcal{D} , such that all spherical faces are simultaneously approximated as,

$$S \approx \Phi_I \cdot C. \quad (3)$$

The matrix $C \in R^{K \times n}$ holds the coefficient vectors (in its columns) and $\Phi_I = [g_{\gamma_1}, \dots, g_{\gamma_K}]$.

The coefficient vector conveys quite discriminative information about the faces signals. However, the class separability of the coefficient vectors in the reduced space could yet be improved by performing an optional Linear Discriminant Analysis (LDA) step before matching. LDA exploits the class labels information of the training samples in order to enhance the discriminant properties of the coefficient vectors. It introduces supervision in the recognition process and permits to build a new set of coefficient vectors $\tilde{C} = CW$ where the weights W are chosen to optimize the ratio of between-class variance and within-class variance for training data [10].

Finally, the matching is performed by comparing the coefficient vectors C , which represent the lower dimensional data samples. The recognition is performed by nearest neighbor classification. We iteratively compute the coefficients c_t of the test face signal s_t on the sub-dictionary \mathcal{D}_I . The classification is then performed by computing the L_1 distance between c_t and any coefficient vector c_i corresponding to the training signals

$$d(c_t, c_i) = \sum_{j=1}^K |c_t(j) - c_i(j)|. \quad (4)$$

The class of the test signal is finally given by the class of the signal s_i that leads

Test configuration	i	Number of subjects	Training set	Test set
T_1	1	200	200	673
T_2	2	166	332	474
T_3	3	121	363	308
T_4	4	86	344	187

Table 1: Test configurations and their characteristics.

to the smallest distance $d(c_t, c_i)$ between the coefficients vectors. The same classification method is used for coefficients \tilde{C} modified by LDA. The choice of the L_1 distance metric is mostly empiric as it leads to superior classification performance compared to other metrics.

5. Experimental results

5.1. Experimental setup

In this section, we evaluate the performance of the proposed algorithms in both recognition and verification scenarios. We compare our algorithms with PCA and LDA on depth images that have undergone the same preprocessing step as the data used in the SSMP algorithm. PCA and LDA are well known methods that represent state-of-the-art technologies for 3D recognition.

For our evaluation, we use the UND (University of Notre Dame) Biometric database [29, 30], also known as FRGC v.1.0 database. It contains 953 facial images of 277 subjects, where each subject has between one and eight scans. Each facial scan is provided in the form of a 3D point-cloud, along with a corresponding binary matrix of valid points. The number of vertices in a point-cloud typically varies between 30.000 and 40.000.

We defined several test configurations for our experimental evaluation. Each configuration is characterized by the number of samples per subject that form the training set. For each configuration T_i , we keep only the subjects from the

database that have at least $i + 1$ samples, and we use i training samples per class (randomly chosen), while assigning the rest to the test set. The subjects that have only one facial scan can not be used in the recognition tests. Table 1 summarizes the test configurations and their main characteristics.

SSMP implementation. For the dictionary construction in SSMP-based methods, we have used the 2D Gaussian on the sphere (1) as the generating function. The atom indexes γ that define the dictionary, have to take discrete values in practice. We use here a discretization of the dictionary as in [28], mostly built on empirical choices for atom parameter values. The position parameters, τ and ν are uniformly distributed on the interval $[0, \pi]$, and $[-\pi, \pi)$, respectively, with equal resolution of 128 points. The rotation parameter ψ is uniformly sampled on the interval $[-\pi, \pi)$, with the same resolution as τ and ν . This choice is mostly due to the use of fast computation of correlation on SO(3) for the full atom search within the SSMP algorithm. In particular, we used the *SpharmonicKit* library¹, which is part of the *YAW toolbox*². Finally, scaling parameters are distributed in a logarithmic manner, from 1 to half of the resolution of τ and ν , with a granularity of one third of octave. The largest atom covers half of the sphere.

The use of fast computation of correlation on the SO(3) group requires the spherical data to be sampled on an equiangular (θ, φ) grid, defined as:

$$G = \{(\theta_i, \varphi_j), \theta_i = \frac{(2i + 1)\pi}{2N_\theta}, \text{ and } \varphi_j = \frac{j2\pi}{N_\varphi}\}. \quad (5)$$

where: $i = 0, \dots, N_\theta - 1$ and $j = 0, \dots, N_\varphi - 1$. Since 3D face point clouds are projected as scattered data on the sphere, an interpolation step is necessary. For its simplicity we use k-nearest neighbor interpolation, where the value on each spherical grid point (θ_i, φ_j) is computed as an average of its k nearest neighbors. We have used $k = 4$ and a resolution of $N_\theta = 128, N_\varphi = 128$. Note finally that, for the sake of computational ease, dimensionality reduction

¹<http://www.cs.dartmouth.edu/~geelong/sphere/>

²<http://fyma.fy.ma.ucl.ac.be/projects/yawtb/>

with SSMP is performed off-line, using only one training face per subject. The resulting subspace is then used for projecting both training and test samples.

Virtual faces. The size of the training set is important in determining the classification performance. We propose to enrich the training set with *virtual faces* (see e.g., [31] and references therein). These are faces that are artificially generated by slight variations of the original training faces. They are given the corresponding class labels of the training face they originate from, and they are treated as training samples. The use of virtual faces is motivated by two main reasons: (i) they compensate for small registration errors (recall that our registration process is fully automatic and it is expected to contain a few registration errors) and (ii) by augmenting the training set, they may contribute to the performance of sample-based methods (e.g., LDA) that can benefit from large sample sets. Note that the virtual faces do not introduce any new information to the training set, since they are synthetically generated by the original training faces. For computational convenience, we construct them by one or two pixel translations in the spherical domain. Note finally that virtual faces are used only in the SSMP+LDA method.

5.2. Recognition results

We present recognition results of our methods and we compare them with PCA and LDA on depth images. For the sake of completeness, we also report the classification performances of the Euclidean distance (EUC) between depth images, and Mean Square Error (MSE) between spherical functions. For the two latter methods, each test face is recognized as the closest neighbor in the training set. In SMMP+LDA (resp. PCA+LDA), the number of dimensions used in LDA is set to the minimum between the number of features in SSMP (resp. PCA) and $c - 1$, where c is the number of classes (subjects). Virtual faces are used in the SSMP+LDA method in configurations T_1 , T_2 and T_3 only, since they correspond to small training sets. In these cases, each training face is used to generate 8 virtual faces.

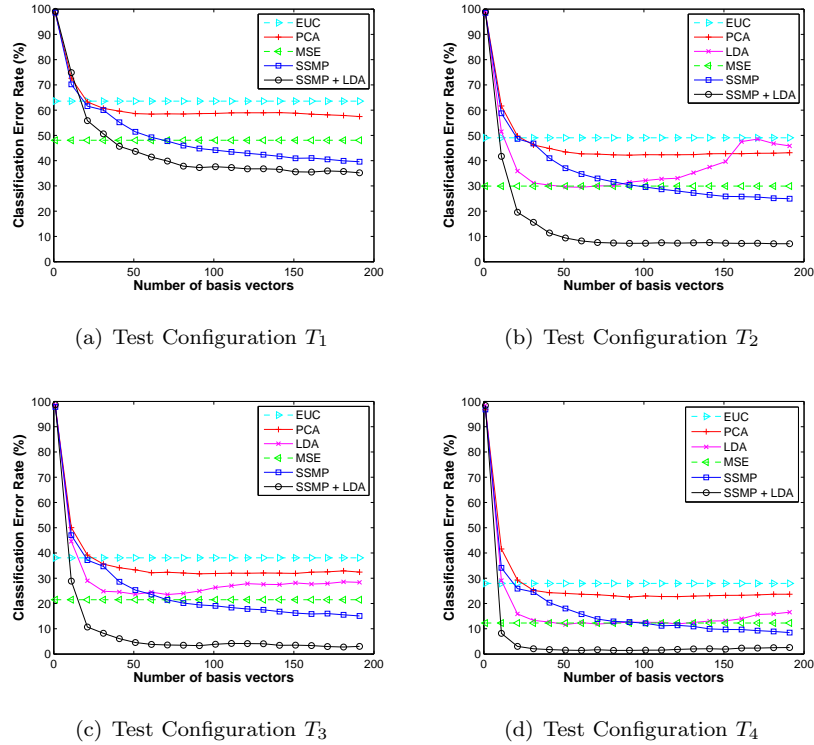


Figure 7: Rank-1 recognition results: average classification error rate versus the dimension of the subspace.

We start with rank-1 recognition, which refers to the scenario where a class prediction is considered to be a hit when the label of the closest neighbor is the correct one. Then, we will discuss the generic rank- k scenario, where the prediction is a hit when the correct label is included in the labels of the closest k neighbors.

Rank-1 recognition. All tests are performed 10 times, by splitting randomly the samples into the training and the test sets. Figure 7 shows the classification error rate for all configurations, averaged over the 10 random experiments. Notice the remarkable improvement introduced by the employment of spherical functions for facial representation. This is evident from the fact that the recognition performance of nearest neighbor classification with Mean Square Error

	T_1	T_2	T_3	T_4
PCA	45,17	60,97	74,35	82,89
PCA + LDA	-	74,89	80,52	93,58
SSMP	62,85	77,22	87,01	94,12
SSMP + LDA	67,61	94,73	98,70	100

Table 2: Best rank-1 recognition rates (%) reached by each method in experiment 5.2.

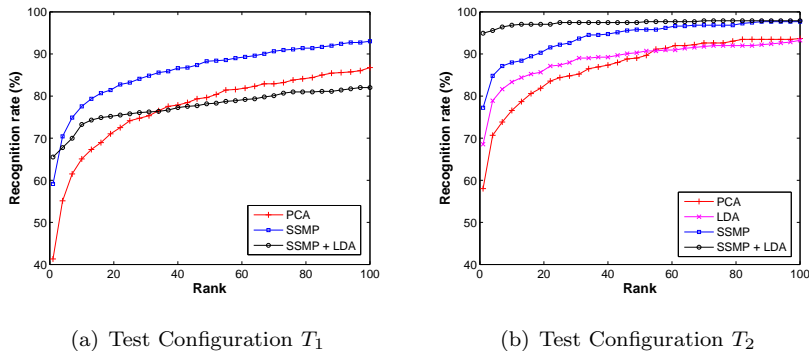


Figure 8: Rank- k recognition results in terms of CMC curves.

(MSE) between spherical signals, outperforms that of Euclidean distances between depth images (EUC). This provides also the main motivation for working on the sphere. Based on this observation, it seems reasonable that our SSMP algorithm outperforms PCA in all configurations. Notice finally that SSMP+LDA is the best performer. In T_2 , SSMP reaches recognition performance of 77,22%, while SSMP+LDA reaches 94,73%. The latter goes to the maximum 100% in T_4 , even in the absence of virtual faces. Table 2 shows the highest recognition rates achieved by each method in all configurations.

Rank- k recognition. We report rank- k recognition performances in terms of cumulative match characteristic (CMC) curves. A CMC curve simply illustrates the fluctuation of the recognition rate versus the rank k . Figure 8 shows the obtained CMC curves for T_1 and T_2 that represent the most interesting cases,

since T3 and T4 correspond to very good performances for all methods. The CMC curves in this figure are averages over 10 random tests, where the best number of dimensions for each algorithm is used (obtained from the previous rank-1 recognition experiments). As expected, notice again that SSMP is superior to PCA, and LDA introduces in both methods a significant performance boost.

5.3. Verification results

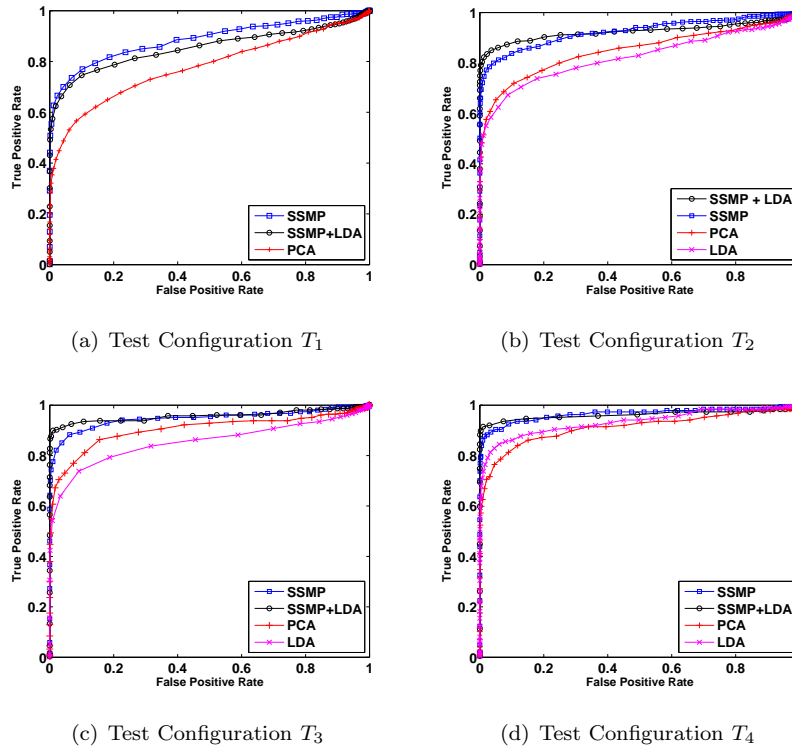


Figure 9: Verification performance in terms of ROC curves.

We compare now all the above methods in the verification scenario, where the test subject claims an identity and the system has to either accept or reject this claim. If the identity is the correct one, then the test subject is called a *client*; otherwise, it is called an *impostor*. In systems that output a confidence score

about the test subject, a hard decision (i.e., accept or reject) is typically reached according to a threshold value. We report the verification performances in terms of receiver operating characteristic (ROC) curves, which show the fluctuation of the true positive rate (TPR) versus the false positive rate (FPR) across all values of the threshold. For the computation of the ROC curve we consider every possible pair of subject and claimed identity.

In our experimental setup, we use the dimensions that yields the best performance, which corresponds to 200 atoms in SSMP and 100 dimensions in PCA. The number of LDA dimensions in both SSMP+LDA and PCA+LDA is set with the same rule as in the recognition experiments (i.e., using the minimum between the number of PCA/SSMP features and $c - 1$). Also, in SSMP+LDA we use virtual faces only for configurations T1 and T2. Figure 9 shows the average ROC curves over 10 random experiments for all configurations. Similar conclusions can be drawn here as well. Unsurprisingly, observe again that SSMP consistently outperforms PCA in all configurations and SSMP+LDA is the best performer.

5.4. Discussion

It is worth noting that supervised versions of SSMP could be also used [25]. The idea would be then to select the atoms from the dictionary according to discriminative criteria. However, in the proposed scheme the supervision information is already taken into account in the LDA postprocessing step, and prior experience has shown that this suffices, when predefined dictionaries are used.

Note also that the importance of each region of the face in terms of recognition performance is certainly not uniform [17]. Although the selection of such regions is typically performed manually and it maybe sensitive to the testing conditions, one possible approach to take advantage of this observation could be to group the features selected by SSMP into regions by clustering on the sphere, do a classification per region and then fuse the results (e.g., by majority voting). Such an approach however requires a sufficient number of atoms in each area,

and the performance of such a region-based classifier has not been convincing.

Note finally that the proposed dimensionality reduction scheme is generic and simple extensions could be proposed to make the classification more sensitive to some specific areas. For example, the SSMP scheme can easily be adapted to give priorities to regions of high interest such as the nose or the eyes. Such a prioritization can be achieved by giving proper weights to atoms located in different areas, in order to force the dimensionality reduction step to select features in areas that are expected to be more discriminative. This however goes along the lines of supervised versions of SSMP mentioned above with the main difference that discriminative capability in this case is mostly defined in a region-based way.

6. Conclusions

We have proposed a methodology for 3D face recognition based on spherical sparse representations. First, we introduced a fully automatic process for extraction, preprocessing and registration of facial information in 3D point clouds. Next, we proposed to convert faces from point clouds to spherical signals. Sparse spherical representation of faces allows for effective dimensionality reduction through simultaneous sparse approximations. The dimensionality reduction step preserves the geometry information, which in turn leads to high performance matching in the reduced space. We provide ample experimental evidence that indicates the advantages of the proposed approach over state-of-the-art methods working on depth images.

7. Acknowledgements

The authors would like to thank Prof. Patrick Flynn for sharing with us the UND Biometrics database.

References

- [1] A. Jain, L. Hong and S. Pankati. “Biometric Identification”. *Communications of the ACM*, vol. 43, no. 2, pp. 90-98. Feb. 2000.
- [2] K.W. Bowyer, K. Chang and P. Flynn. “A survey of approaches and challenges in 3D and multi-modal 3D+2D face recognition”. *Computer Vision and Image Understanding*, vol. 101(1), pp. 1-15, Jan. 2006.
- [3] L. Akarun, B. Gokberk and A.A. Salah. “3D Face recognition for biometric applications”. *Proc. European Signal Processing Conference, Antalya 2005*.
- [4] P. Besl and N. McKay. “A method for registration of 3D shapes”. *IEEE Trans. on Pattern Analysis and Machine Intelligence*, vol. 14, pp. 239-256. 1992.
- [5] I.T. Jolliffe. *Principal Component Analysis*. Springer Verlag, New York, 1986.
- [6] B. Gökberk, M.O. Irfanoğlu and L. Akarun. “3D shape-based face representation and feature extraction for face recognition”. *Image and Vision Computing*, vol. 24, pp. 857-869. 2006.
- [7] B. Achermann and H. Bunke. “Classifying range images of human faces with Hausdorff distance”. *15-th International Conference on Pattern Recognition*, pp. 809-813, Sept. 2000.
- [8] C. Xu, Y. Wang, T. Tan and L. Quan. “A new attempt to face recognition using 3D Eigenfaces”. *Proceedings of the Asian Conference on Computer Vision*. (2) 884-889. 2004.
- [9] M.A. Turk and A.P. Pentland. “Face recognition using Eigenfaces” . Vision and Modeling Group, The Media Laboratory Massachusetts Institute of Technology. 1996.
- [10] P.N. Belhumeur, J.P. Hespanha and D.J. Kriegman. “Eigenfaces vs. Fisherfaces: recognition using class specific linear projection” *IEEE Trans. on Pattern Analysis and Machine Intelligence.*, vol. 19, no. 7, July 1997.
- [11] D.D. Lee and H.S. Seung. “Algorithms for non-negative matrix factorization”. *Advances in Neural Information Processing Systems (NIPS)*, vol. 13, pp. 556-562, 2001.

- [12] P. Paatero and U. Tapper. "Positive matrix factorization: A non-negative factor model with optimal utilization of error estimates of data values". *Environmetrics*, vol. 5, pp. 11-126. 1994.
- [13] P.O. Hoyer, "Non-negative matrix factorization with sparseness constraints". *Journal of Machine Learning Research*, vol. 5, pp. 1457-1469, 2004.
- [14] P. O. Hoyer, "Non-negative sparse coding", IEEE Workshop on Neural Networks for Signal Processing, pp. 557-565, 2002.
- [15] B.J. Shastri and M.D. Levine. "Face recognition using localized features based on non-negative sparse coding". *Machine Vision and Applications*. vol. 18, pp. 107-122, 2007.
- [16] S. Jahanbin, H. Choi, A.C. Bovik and K.R. Castleman "Three dimensional face recognition using wavelet decomposition of range images" *International Conference on Image Processing*, pp.145-148, Sep. 2007.
- [17] K. Wong, W. Lin, Y. Hu and N. Boston, "Optimal linear combination of facial regions for improving identification performance". *IEEE Trans. on Systems, Man, and Cybernetics - Part B: Cybernetics*, vol. 37, no. 5, Oct. 2007.
- [18] S. Gupta, J.K. Aggarwal, M.K. Markey and A.C. Bovik, "3D face recognition founded on the structural diversity of human faces", IEEE Conf. on Comp. Vis. and Patt. Rec. (CVPR), June 2007.
- [19] G. Gordon. "Face recognition based on depth and curvature features". *SPIE Proc. Geometric methods in Computer Vision*, vol. 1570, pp. 234-247, 1991.
- [20] C. Samir, A. Srivastava and M. Daoudi. "Three-dimensional face recognition using shapes of facial curves" *IEEE Trans. on Pattern Analysis and Machine Intelligence*, vol. 28, no. 11, Nov. 2006.
- [21] H. Wang, H. Wei and Y. Wang, "Face representation under different illumination conditions". *IEEE Int. Conf. on Multimedia & Expo (ICME)* pp.285-288, 2003.
- [22] R. Ramamoorthi. "Analytic PCA construction for theoretical analysis of lighting variability in images of a Lambertian object". *IEEE Trans. on Pattern Analysis and Machine Intelligence*, vol. 24, no. 10, Oct. 2002.

- [23] Z. Yue, W. Zhao and R. Chellappa. “Pose-encoded spherical harmonics for face recognition and synthesis using a single image”. *EURASIP Journal on Advances in Signal Processing*. 2008.
- [24] M. Hebert, K. Ikeuchi and H. Delingette. “A spherical representation for recognition of free-form surfaces”. *IEEE Transactions on Pattern Analysis and Machine Intelligence*. vol.17, no.7, July 1995.
- [25] E. Kokioppoulou and P. Frossard. “Semantic coding by supervised dimensionality reduction” *IEEE Transactions on Multimedia*, vol. 10, no. 5, pp. 806-818, August 2008.
- [26] S.G. Mallat and Z. Zhang. “Matching pursuit with time-frequency dictionaries”, *IEEE Trans. on Signal Processing*, vol. 41, no. 12, pp. 3397-3415, Dec. 1993.
- [27] J. Tropp, A. Gilbert, and M. Strauss. “Algorithms for simultaneous sparse approximation. Part I: Greedy pursuit”, *Signal Processing, special issue “Sparse approximations in signal and image processing”*, vol. 46, pp. 572-588, April 2006.
- [28] I. Tomic, P. Frossard and P. Vandergheynst. “Progressive coding of 3D objects based on overcomplete decompositions” *IEEE Transactions on Circuits and Systems for Video Technology*, vol. 16, no. 11, pp. 1338-1349, Nov. 2006.
- [29] P. J. Flynn, K. W. Bowyer, and P. J. Phillips, “Assessment of time dependency in face recognition: An initial study”, *Audio and Video-Based Biometric Person Authentication*, pp.44-51, 2003.
- [30] X. Chen, P. J. Flynn, and K. W. Bowyer, “Visible-light and infrared face recognition”, *ACM Workshop on Multimodal User Authentication*, pp.48-55, December 2003.
- [31] D. DeCoste and M.C. Burl, “Distortion-invariant recognition via jittered queries”, *IEEE Int. Conf. on Computer Vision and Pattern Recognition (CVPR)*, 2000.